

Theoretical explanation of the uniform compressibility behavior observed in oxide spinels

J. M. Recio, R. Franco, A. Martín Pendás, M. A. Blanco, and L. Pueyo
Departamento de Química Física y Analítica, Universidad de Oviedo, E-33006 Oviedo, Spain

Ravindra Pandey

Department of Physics, Michigan Technological University, Houghton, Michigan 49931

(Received 26 October 2000; published 6 April 2001)

Simple algebraic equations show that the bulk compressibility in spinel-type compounds can be expressed by means of cation oxide polyhedral compressibilities and a term that accounts for the pressure effect on the internal oxygen position in the unit cell. The equations explain (i) the difference of compressibilities at octahedral and tetrahedral sites, (ii) why the macroscopic bulk modulus can be estimated as the average of these polyhedral bulk moduli, and (iii) the uniform behavior found in oxide spinels under hydrostatic pressure. Quantum-mechanical *ab initio* perturbed ion results on MgAl_2O_4 , ZnAl_2O_4 , ZnGa_2O_4 , and MgGa_2O_4 direct spinels and on MgGa_2O_4 inverse spinel are reported to illustrate the interpretative capabilities of the proposed equations.

DOI: 10.1103/PhysRevB.63.184101

PACS number(s): 64.30.+t, 82.20.Wt

I. INTRODUCTION

The understanding of crystalline bulk properties in terms of simple contributions has traditionally demanded the development of new empirical relationships and theoretical models. This basic investigation is of general importance because the derived equations permit to access to conditions and materials where the information is unknown. In geosciences, the interest in the description and prediction of mineral compression has led to the interpretation of crystal bulk moduli in terms of the bulk moduli of the cation-anion constitutive polyhedra.¹ Hazen and Finger gave empirical expressions for polyhedra compressibilities analogous to those derived for the crystal bulk modulus by Bridgman² and Anderson and co-workers.^{3,4} The use of these expressions, along with information on the nature of the polyhedra linkages, enables the estimation of the macroscopic compressibility for a large variety of crystalline materials.

Concerning spinel-type compounds, Hill *et al.*⁵ systematized their structural properties by means of empirical expressions that involve the ionic size as the controlling parameter. They derived an exact relation that connects the oxygen u coordinate in the unit cell with the ratio of the octahedral to tetrahedral cation-oxygen bond lengths. The equation informs on the different compressibility behavior at the two interstices once the u response to hydrostatic pressure is known. Based on some of the results of that work, Finger *et al.*⁶ explored the observed bulk modulus of several oxide spinels and found “intriguing” that the average of the tetrahedral and octahedral bulk moduli were in a very good agreement with the crystal bulk modulus. These authors suggested that *all* oxide spinels may have a similar bulk modulus around 200 GPa. In fact, values of 196 ± 1 , 206 ± 4 , and 197 ± 5 have been recently measured for MgAl_2O_4 , NiMn_2O_4 , and ZnMn_2O_4 , respectively (see Refs. 7–9).

It is our basic aim in this paper to contribute to the understanding of the reasons that explain the similar compressibilities exhibited by a number of oxide spinels. We develop simple analytic relationships between polyhedral and bulk

compressibilities that involve also the oxygen u coordinate and its dependence on hydrostatic pressure. The performance of the equations is manifested through the results obtained in AB_2O_4 ($A = \text{Mg, Zn}$; $B = \text{Al, Ga}$) direct spinels (where u is a decreasing function of pressure) and MgGa_2O_4 inverse spinel (where u is an increasing function of pressure). Calculations in these compounds have been performed using the *ab initio* perturbed ion (*aiPI*) model, a localized Hartree-Fock approach that solves the Schrödinger equation of the crystal by breaking the total wave function into ionic monocentric contributions.¹⁰

As a second product of our investigation, we provide theoretical data on the structural and equation of state (EOS) parameters of these compounds that are compared with the sparing available experimental and theoretical information. The rest of the paper contains (i) derivation of the analytical expressions (Sec. II), (ii) the results and discussion (Sec. III), which includes the computational model, the EOS of the five spinels, and the decomposition of the macroscopic compressibility according to the proposed equations, and (iii) a summary of the main findings and conclusions of this work (Sec. IV).

II. ANALYTICAL RELATIONSHIPS FOR POLYHEDRAL COMPRESSIBILITIES

For a better understanding of the rest of the paper, we include here the information on the setting we adopt for the AB_2O_4 spinel unit cell. It contains 56 atoms, being the space group $Fd\bar{3}m$. The oxygen is located at (u, u, u) forming a distorted face-centered-cubic structure. The A cations are at $(\frac{1}{8}, \frac{1}{8}, \frac{1}{8})$ positions, occupying 8 of the 64 tetrahedral interstices in the direct spinel, and the B cations are at $(\frac{1}{2}, \frac{1}{2}, \frac{1}{2})$ positions, occupying 16 of the octahedral interstices in the direct spinel. For the inverse spinel structure, half of the B cations go to the tetrahedral positions, whereas the A cations go to octahedral interstices.

According to this definition of the unit cell, the following

general equations for spinel-type structures are easily obtained:¹¹

$$V = \frac{a^3}{8}; \quad V_{\text{tet}} = \frac{64}{3} V \left(u - \frac{1}{8} \right)^3, \quad V_{\text{oct}} = \frac{128}{3} V \left(u - \frac{3}{8} \right)^2 u, \quad (1)$$

$$d_{A-O} = \sqrt{3} a \left(u - \frac{1}{8} \right), \quad d_{B-O} = a \sqrt{\left(u - \frac{1}{2} \right)^2 + 2 \left(u - \frac{1}{4} \right)^2}, \quad (2)$$

where, V , V_{tet} , and V_{oct} stand, respectively, for the molecular, tetrahedral, and octahedral volumes; a is the lattice parameter of the cubic unit cell, and d_{A-O} and d_{B-O} are the cation-anion bond lengths at the tetrahedral and octahedral interstices, respectively. It is to be noted that the occupied tetrahedra are regular regardless the value of u , and therefore V_{tet} can be expressed using only the d_{A-O} variable. However, the occupied octahedra are distorted (only at $u=0.25$ are regular) and the V_{oct} expression in terms of d_{B-O} includes also the u variable.

We define the isothermal tetrahedral and octahedral bulk moduli, B_{tet} and B_{oct} , by

$$B_{\text{tet}} = -V_{\text{tet}} \left(\frac{\partial P}{\partial V_{\text{tet}}} \right)_T, \quad B_{\text{oct}} = -V_{\text{oct}} \left(\frac{\partial P}{\partial V_{\text{oct}}} \right)_T, \quad (3)$$

being their corresponding compressibilities

$$\kappa_{\text{tet}} = \frac{1}{B_{\text{tet}}}, \quad \kappa_{\text{oct}} = \frac{1}{B_{\text{oct}}}, \quad (4)$$

which in terms of the bulk compressibility κ and the u parameter and its pressure derivative are

$$\kappa_{\text{tet}} = \kappa - \frac{3}{u - \frac{1}{8}} \left(\frac{\partial u}{\partial P} \right)_T, \quad \kappa_{\text{oct}} = \kappa - \left(\frac{2}{u - \frac{3}{8}} + \frac{1}{u} \right) \left(\frac{\partial u}{\partial P} \right)_T. \quad (5)$$

Thus, the average of the polyhedral compressibilities $\bar{\kappa}$ is

$$\bar{\kappa} = \kappa - \frac{1}{2} \left(\frac{\partial u}{\partial P} \right)_T \left(\frac{3}{u - \frac{1}{8}} + \frac{2}{u - \frac{3}{8}} + \frac{1}{u} \right) \quad (6)$$

and contains the ingredients to explain the ‘‘intriguing’’ similarities between the κ and $\bar{\kappa}$ values. Also, the difference between κ_{oct} and κ_{tet} is given by

$$\kappa_{\text{oct}} - \kappa_{\text{tet}} = \frac{3(8u+1)}{u(8u-3)(1-8u)} \left(\frac{\partial u}{\partial P} \right)_T. \quad (7)$$

As the first factor is positive for the physical meaningful range of u values⁵ ($0.25 < u < 0.274$), the sign of the difference is therefore controlled by that of the slope of the u vs P curve.

III. RESULTS AND DISCUSSION

A. Computational model

The total energies of MgAl_2O_4 , ZnAl_2O_4 , ZnGa_2O_4 , and MgGa_2O_4 direct spinels, and MgGa_2O_4 inverse spinel have been computed by means of the *aiPI* method.¹⁰ Multi- ζ Slater-type orbitals basis sets from Clementi and Roetti¹² have been used for trivalent and divalent cations. For O^{2-} , the O^- basis set has been chosen. Correlation energy corrections are introduced through the Coulomb-Hartree-Fock model of Chakravorty and Clementi.¹³ Details of the method can be found in Refs. 10 and 14. Modelization of the inverse spinel is carried out by assigning fractional occupancies of $\frac{1}{2}$ to Ga^{3+} and Mg^{2+} at the octahedral positions.

As in previous *aiPI* calculations,¹⁵ the computational strategy consists in the evaluation of the total energy at selected volumes covering a wide interval containing the equilibrium geometry. At each volume, the internal parameter u is optimized to give the minimum total energy following a conjugate gradient algorithm. This procedure provides the dependence of the total energy on volume, which serves as input for the determination of the EOS.¹⁶ Once the pressure vs volume relationship is obtained, V_{oct} and V_{tet} values can be assigned to different pressures. This information allows us to fit standard analytical EOS to generate the polyhedral bulk moduli. In our study, we have used Birch¹⁷ and Vinet *et al.*¹⁸ forms, and we have found consistency in the final EOS parameters.

B. Static equations of state for AB_2O_4 ($A = \text{Mg, Zn}$; $B = \text{Al, Ga}$) spinels

Table I collects zero-pressure results obtained for the five spinels at static conditions along with available room-temperature-observed values from Ref. 5. B_0 and B'_0 experimental data are lacking except for MgAl_2O_4 ,⁷ and we have opted to include recent theoretical values also.^{19,20} The selection of these four direct spinels allows us to investigate trends affected only by the progressive substitution of just one cation. This clarifies the discussion. Consideration of the inverse MgGa_2O_4 spinel is justified by two reasons. First, it is expected from the observed disorder parameter that MgGa_2O_4 behaves close to the inverse limit. Second, the effect of hydrostatic pressure on inverse spinels yields a different response of the internal parameter with respect to that found in direct ones due to the different occupancies of tetrahedral and octahedral interstices. This fact enriches the analysis of the equations proposed here.

The athermal computed lattice parameters are around 4% smaller than the observed data. The increase of a from Al to Ga spinels is captured in the calculations up to 0.10–0.15 Å, whereas the corresponding observed values lie around 0.20–0.25 Å. Roughly, these spinels present analogous lattice spacings, the variations being lower than 3%. The computed u parameter is overestimated by about 2% with respect to the tabulated data of Hill *et al.*⁵ The a and u discrepancies are translated to the cation-oxygen distances that show disagreements around 5% with the experiments,

TABLE I. Zero-pressure structural properties of MgAl_2O_4 , ZnAl_2O_4 , MgGa_2O_4 , and ZnGa_2O_4 according to *ai*PI-uCHF (unrelaxed Coulomb-Hartree-Fock) calculations (first rows) and other data available (second rows). Lengths in Å, u in fractional units, and B_0 in GPa.

	MgAl_2O_4	ZnAl_2O_4	ZnGa_2O_4	MgGa_2O_4	MgGa_2O_4 (inv)
a	7.886	7.835	7.977	8.021	7.969
	8.0832 ^a	8.086 ^a	8.330 ^a	8.270 ^b	8.2800 ^a
u	0.2688	0.2675	0.2673	0.2683	0.2559
	0.2624 ^a	0.2636 ^a	0.2617 ^a	0.2614 ^b	0.2540 ^a
d_{A-O}	1.964	1.934	1.966	1.991	1.946
	1.923 ^a	1.941 ^a	1.972 ^a	1.954 ^b	2.037 ^a
d_{B-O}	1.835	1.832	1.866	1.870	1.946 ^c – 1.807 ^d
	1.926 ^a	1.918 ^a	1.990 ^a	1.978 ^b	2.037 ^{a, c} – 1.850 ^{a, d}
B_0	205.01	206.91	207.52	204.56	215.30
	196 ± 1 ^e	273 ^f	237 ^f	243 ^b – 243 ^f	
B'_0	3.57	3.48	3.77	3.80	3.65
	4.7 ± 0.3 ^e	3.4 ^f	3.5 ^f	3.3 ^b	

^aExperimental values from Ref. 5.

^bCalculated values from Ref. 20.

^cAt octahedral sites.

^dAt tetrahedral sites.

^eExperimental values from Ref. 7.

^fCalculated values from Ref. 19.

being the predictions slightly better for the $A-O$ distances. Overall, we believe that the computed structural data is accurate enough to carry out a reasonable analysis of their dependence on hydrostatic pressure. We should remark at this point that our calculations predict the expected decrease of the u parameter in the inverse spinel (0.2559) relative to the direct ones (~ 0.268). Moreover, the known fact that inverse and direct spinels exhibit opposite u vs P slopes is also manifested in our calculations (see Fig. 1). Direct spinels respond to pressure trying to reach the ideal structure with nondistorted octahedral polyhedra. This phase is characterized by $u = 0.25$, and therefore u decreases with pressure. As inverse spinels is concerned, and since the octahedral interstices are equally shared by divalent and trivalent cations, the concept of ideal structure vanishes, and it is the constraint to keep regular tetrahedra that forces u to increase with pressure.

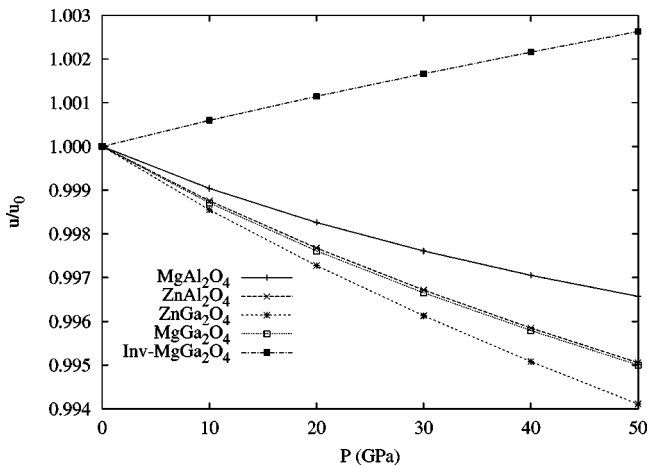


FIG. 1. Reduced u vs pressure diagram for AB_2O_4 spinels ($A:\text{Mg,Zn}; B:\text{Al,Ga}$) according to our calculations. Inv refers to the inverse spinel crystal.

The compressibility of these compounds is directly described by the V/V_0 vs P diagrams (see Fig. 2), being V_0 the zero-pressure volume. These curves show that the four direct spinels essentially behave the same way under hydrostatic pressure. For example, at 10 GPa, the greatest difference in V/V_0 values among the four spinels is less than 6×10^{-4} . At 50 GPa, this difference increases to 4×10^{-3} , but it is still a small quantity. The inverse spinel show a slightly lower compressibility in the pressure range studied here. According to the empirical relationships proposed by Anderson and co-workers,^{3,4} oxide compounds “resemble neither the ionic solids nor the covalent solids.” These authors claimed that B_0 for oxides is virtually the same for a given volume. Our theoretical results confirm the above statement explaining this behavior in terms of the polyhedral compressibilities.

The EOS parameters B_0 and B'_0 are intended to represent the V/V_0 vs P behavior. Our B_0 values inform qualitatively

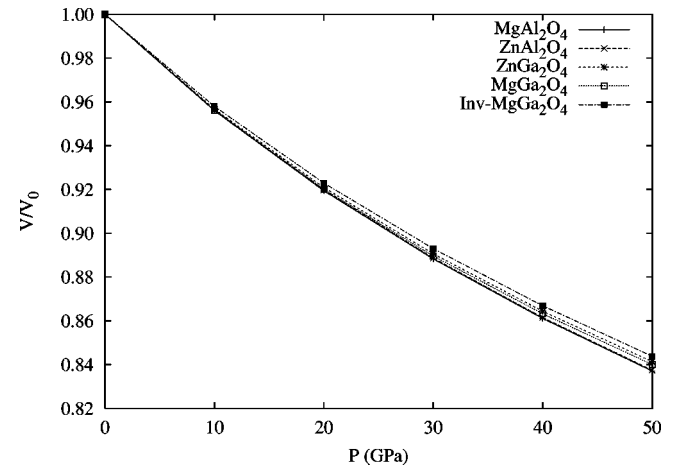


FIG. 2. Reduced volume vs pressure diagram for AB_2O_4 spinels ($A:\text{Mg,Zn}; B:\text{Al,Ga}$) according to our calculations. Inv refers to the inverse spinel crystal.

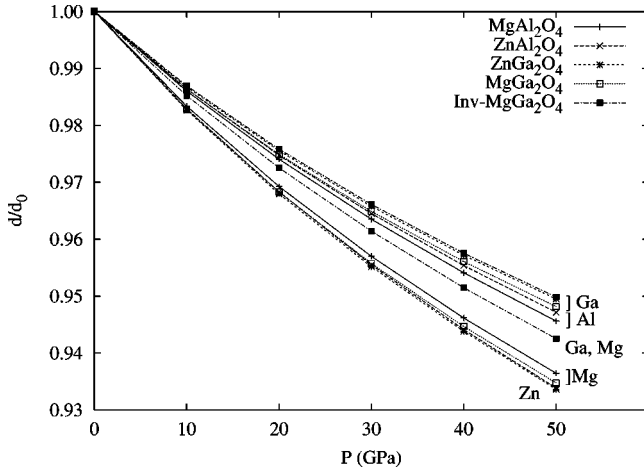


FIG. 3. Reduced cation-oxygen bond lengths vs pressure diagram for AB_2O_4 spinels (A :Mg,Zn; B :Al,Ga) according to our calculations. Inv refers to the inverse spinel crystal.

well that the four direct spinels show similar response to pressure, with common values around 205 GPa. This result also supports Finger *et al.*⁶ speculation of oxide spinels having B_0 around 200 GPa. In order to understand subtle differences among these compounds, B'_0 is also required in the analysis. Computed B_0 values do not follow the order shown by $P - V/V_0$ curves. A correct interpretation of this diagram is recovered taking into account the higher B'_0 values obtained in Ga spinels. Thus, B values at 50 GPa are around 386 GPa for direct $MgGa_2O_4$ and $ZnGa_2O_4$, whereas they decrease down to 370 GPa for $MgAl_2O_4$ and $ZnAl_2O_4$. At this pressure, inverse $MgGa_2O_4$ has $B = 388$ GPa, approaching the compressibility of its corresponding direct spinel.

Comparison of computed B_0 and B'_0 values with other data shows a good agreement in $MgAl_2O_4$, the only case with the experimental information available. For the other three direct spinels, the atomistic values obtained by Pandey *et al.*¹⁹ in $ZnAl_2O_4$ and $ZnGa_2O_4$, and the pseudopotential Hartree-Fock calculations²⁰ in $MgGa_2O_4$ lie well above our predictions. It is known that the use of rigid interionic potentials usually overestimates B_0 values. It is due to the low flexibility of the potentials in order to describe pressure effects on the ionic interactions. Regarding D'Arco *et al.* calculations, the lack of correlation-energy corrections lead also to an overestimation for B_0 . We should note that their prediction for B_0 in $MgAl_2O_4$ (266 GPa) is quite large as compared to the experimental value (196 ± 1 GPa). It is, therefore, reasonable to conclude that our data give a more realistic picture of the compressibility of the five spinels considered in this study.

C. Bond, polyhedral, and macroscopic compressibilities

The rate at which cation-oxygen bond lengths decrease as pressure is applied is depicted in Fig. 3. For the direct spinel crystals, it is apparent that the curves are grouped by the oxidation state of the cation: oxygen distances to trivalent cations are less compressible than those to divalent ones. This is the expected behavior, and it is in correlation with the

zero pressure bond distance values (see Table I): d_{A-O} is around 1.96 Å, whereas d_{B-O} is around 1.85 Å. We remark here that our results are in agreement with D'Arco *et al.* expectations:²⁰ the compression in these direct spinels is “achieved mostly by deformation of the tetrahedra.” In contrast, Sinha *et al.*²¹ predicted greater force constants for the divalent-oxygen bonds than for the trivalent-oxygen ones in $MgAl_2O_4$ and $ZnGa_2O_4$, after a parametrization of Raman spectrum data. Although a rattling behavior for trivalent cations may be suggested in the direct spinel structures, our results clearly illustrate the dominant role of trivalent cation-oxygen bonds in the compressibility of these compounds.

In the case of the inverse $MgGa_2O_4$ spinel, the tetrahedral interstices are all occupied by Ga^{3+} , and the corresponding Ga-O bond length shows the lowest compressibility. Note also that the tetrahedral d_{Ga-O} distance is the shortest one (1.807 Å). However, the octahedral interstices are equally populated by Mg^{2+} and Ga^{3+} , and are forced to have the same size. Thus, our modeling of the inverse spinel produces the same compressibility for Mg-O and Ga-O bonds, and this crystal behaves between the two groups of curves already mentioned.

Bond-length compressibilities roughly determine polyhedral compressibilities. The relation for tetrahedral polyhedra is direct as V_{tet} can be expressed as a function of the cation-oxygen distance only [see Eqs. (1) and (2)]. It should be emphasized that the tetrahedra are regular in the spinel structure at any u value. On the contrary, the $V_{oct}-d_{B-O}$ relationship involves the u parameter as the octahedra are distorted. Nevertheless, the behavior of u does not modify the qualitative picture found in the analysis of bond compressibilities (see Fig. 4). Thus, the octahedral polyhedra (containing trivalent cations) show lower compressibilities than the tetrahedral ones (containing divalent cations) in the direct spinels: $(B_0)_{oct}$ and $(B_0)_{tet}$ lie within narrow ranges of 225–235 GPa and 175–181 GPa, respectively (see Table II). In the inverse spinel, the tetrahedral polyhedra containing Ga^{3+} show a high bulk modulus [$(B_0)_{tet} = 231$ GPa], although the highest value is now reached by the octahedral polyhedra containing Ga^{3+} in $ZnGa_2O_4$. This is due to the effect of pressure on the u parameter in this crystal (see Fig. 1), which is translated to the V_{oct} vs P curve.

From the above analysis, we can conclude that the influence of the *particular* divalent and trivalent cations considered here is almost negligible if they are located in the interstices corresponding to the direct spinel structure. We would like to remark that what is relevant is the oxidation state of the cation accommodated in the interstice. This determines the size of the polyhedra and their corresponding compressibility. The results may be understood using geometrical arguments (the lower the distance, the greater the bulk modulus), but we prefer the energetic point of view (the higher the oxidation state, the stiffer the bond).

In the case of inverse spinel, $(B_0)_{oct}$ is approximately the average of the polyhedral bulk moduli found in the direct spinel, which we understand as due to the equal occupancy of the octahedral interstices by di and trivalent cations. Thus, the energetic considerations seem to be more appropriate in the explanation of this behavior, since the use of the geo-

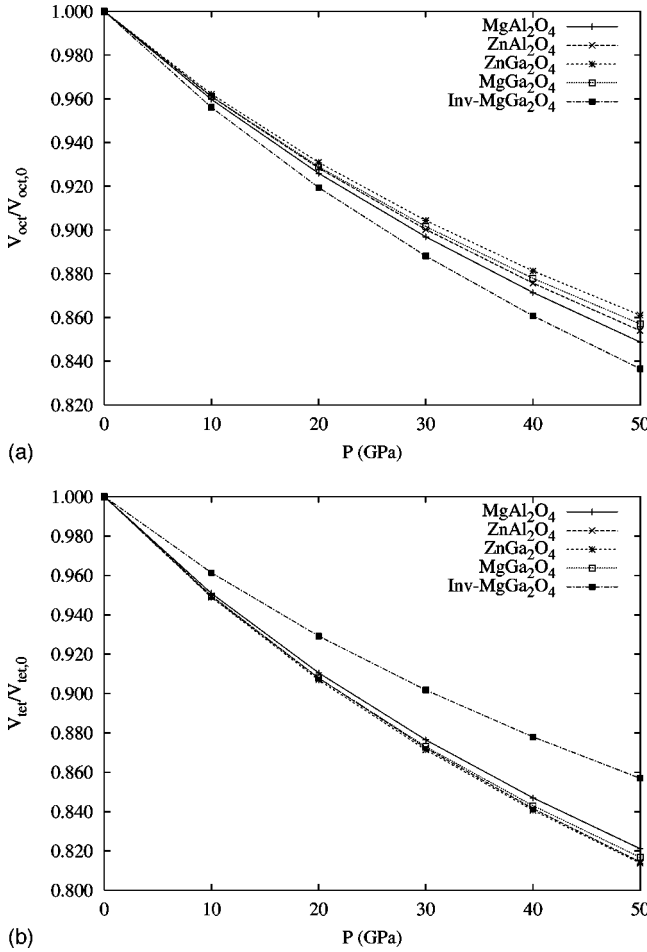


FIG. 4. Reduced polyhedral volumes vs pressure diagram for AB_2O_4 spinels (A :Mg,Zn; B :Al,Ga) according to our calculations. Inv refers to the inverse spinel crystal.

metrical criterium would suggest a lower value for $(B_0)_{oct}$ in the inverse $MgGa_2O_4$ spinel. Besides, $(B_0)_{tet}$ takes the value of $(B_0)_{oct}$ from that of the direct spinel. Our explanation here is again based on the fact that both sites (tetrahedral in the inverse spinel and octahedral in the direct structure) are occupied by trivalent cations, and the cation-oxygen distances in both polyhedra are very similar.

The differences between $(B_0)_{tet}$ and $(B_0)_{oct}$ can be quantitatively explained by means of Eqs. (4) and (7). It is obvious that $(B_0)_{oct}$ is greater than $(B_0)_{tet}$ if u decreases as P is applied. This is the behavior found in the four direct spinels (see Fig. 1). The highest splitting is found in $ZnGa_2O_4$, where the slope of the u vs P curve presents the lowest value. For the inverse spinel, u increases with increasing pressure (see Fig. 1) and, therefore, $(B_0)_{oct}$ is lower than $(B_0)_{tet}$. The difference between $(B_0)_{oct}$ and $(B_0)_{tet}$ is around 55–60 GPa for all direct spinels except $MgAl_2O_4$, which presents a value close to 45 GPa. In the inverse spinel, this difference is –25 GPa.

According to Hazen and Finger bulk modulus-volume relationship for polyhedra,¹ the $(B_0)_{p1}/(B_0)_{p2}$ ratio can provide information on the different ionicity of cation-oxygen bonds in polyhedra of types $p1$ and $p2$:

$$\frac{(B_0)_{p1}}{(B_0)_{p2}} = \frac{z_{p1}}{z_{p2}} \frac{d_{p2}^3 S_{p1}^2}{d_{p1}^3 S_{p2}^2}, \quad (8)$$

where z_{p1} and z_{p2} , d_{p1} and d_{p2} , and S_{p1} and S_{p2} are, respectively, the cation charges, the oxygen-cation bond lengths, and the ionicity parameters of the two polyhedra.

We can express $S_{p1} = \lambda S_{p2}$ in order to compare this ionicity measure of cation-oxygen bonds in two different situations. Using the calculated bond lengths collected in Table I, and the polyhedral bulk moduli of Table II, λ has been evaluated considering that $p1$ and $p2$ are, respectively: (i) the tetrahedral and octahedral polyhedra of the direct spinels ($\lambda = 1.18$), (ii) the Ga and Al octahedral polyhedra ($\lambda = 1.036$), (iii) the Mg and Zn tetrahedral polyhedra ($\lambda = 1.025$), (iv) the Al octahedral polyhedra in $MgAl_2O_4$ and $ZnAl_2O_4$ ($\lambda = 1.010$), (v) the Ga octahedral polyhedra in $MgGa_2O_4$ and $ZnGa_2O_4$ ($\lambda = 1.010$), (vi) the Mg tetrahedral polyhedra in $MgAl_2O_4$ and $MgGa_2O_4$ ($\lambda = 1.003$), (vii) the Zn tetrahedral polyhedra in $ZnAl_2O_4$ and $ZnGa_2O_4$ ($\lambda = 1.016$), and (viii) the Ga octahedral polyhedra in the direct $MgGa_2O_4$ spinel and the Ga tetrahedral polyhedra in the inverse $MgGa_2O_4$ spinel ($\lambda = 1.048$). The analysis of the results can be summarized as follows: (a) in spite of the increase of the coordination number in passing from tetrahedral to octahedral environment, the nominal charge of

TABLE II. Polyhedral and bulk values of B_0 and B'_0 for $MgAl_2O_4$, $ZnAl_2O_4$, $MgGa_2O_4$, and $ZnGa_2O_4$ according to *ai*PI-uCHF calculations. The average \bar{B}_0 and \bar{B}'_k bulk moduli are defined in the text. In brackets separation from B_0 . Units in GPa.

	$MgAl_2O_4$	$ZnAl_2O_4$	$ZnGa_2O_4$	$MgGa_2O_4$	$MgGa_2O_4$ (inv)
B_0	205.01	206.91	207.52	204.56	215.30
B'_0	3.57	3.48	3.77	3.80	3.65
$(B_0)_{oct}$	225.02	231.16	234.58	228.70	205.32
$(B'_0)_{oct}$	3.78	4.09	4.89	4.66	3.56
$(B_0)_{tet}$	181.14	177.88	174.61	174.89	230.65
$(B'_0)_{tet}$	3.52	3.14	3.27	3.50	4.53
\bar{B}_0	203.08 (-1.93)	204.52 (-2.39)	204.60 (-2.92)	201.80 (-2.76)	217.99 (+2.69)
\bar{B}'_k	200.71 (-4.30)	201.50 (-5.86)	200.20 (-7.32)	198.21 (-6.35)	217.25 (+1.95)

the cations makes the divalent cation-oxygen bond to be more ionic than the trivalent cation-oxygen bond, (b) the Ga-O bond is slightly more ionic than Al-O bond, (c) the Mg-O bond is slightly more ionic than Zn-O bond, (d) the cation-oxygen bond character is transferable among the different spinels, and (e) Ga-O bond shows a greater ionic character in the sixfold coordination than in the fourfold coordination environment.

The average of $(B_0)_{\text{oct}}$ and $(B_0)_{\text{tet}}$ (denoted by \bar{B}_0) gives a good estimation of B_0 , as shown in Table II. From Eq. (6), we can define another average for B_0 as the inverse of $\bar{\kappa}$. We represent this quantity by \bar{B}_{0_k} . Values of \bar{B}_{0_k} are also collected in Table II. The reason why \bar{B}_{0_k} and \bar{B}_0 are so similar is the small value of the ratio $(B_{\text{oct}})/(B_{\text{tet}})$ relative to (B_{oct}) or (B_{tet}) . Thus, understanding the values obtained for \bar{B}_{0_k} one finds an explanation for the \bar{B}_0 values. It is observed in Eq. (6) that $\bar{\kappa}$ departs from κ due to two factors: the slope of the u vs P curve and a function of the parameter u . This function, evaluated at zero pressure, gives values between 5.75 and 10.03. The slope at zero pressure varies from -2.2×10^{-5} to -3.1×10^{-5} GPa $^{-1}$ in the direct spinels, and has a value of $+1.2 \times 10^{-5}$ GPa $^{-1}$ in the inverse spinel. Therefore, very small (and positive) differences are expected between $\bar{\kappa}$ and κ in direct spinels, and very small (and negative) differences between $\bar{\kappa}$ and κ in the inverse spinels. The same can be said of the differences between B_0 and \bar{B}_{0_k} . It can be concluded that it is the sign and the magnitude of $(\partial u / \partial P)_T$ that determine the difference between B_0 and \bar{B}_0 .

To explain why B_0 is similar in all the direct oxide spinels studied here, let us return again to Eq. (6) and analyze why κ is similar in these crystals. Given that the product $(\partial u / \partial P)_T \times (3/[u - \frac{1}{8}] + 2/[u - \frac{3}{8}] + 1/u)$ has a negligible effect on κ , the question is translated to the behavior of $\bar{\kappa}$. We can find a detailed explanation of the $\bar{\kappa}$ values in terms of κ_{oct} and κ_{tet} . These two magnitudes are the inverse of the corresponding polyhedral bulk moduli that we have discussed above. Polyhedral bulk moduli are understood as little dependent on the *particular* cation they accommodate inside, provided the cation has the same nominal charge. It is the similar size of the respective octahedral and tetrahedral polyhedra (that in turn are charge dependent) that explains the similar compressibilities exhibited by these oxide spinels.

Note that when the size of the polyhedra moves out of the range found in the direct spinels (as in the inverse MgGa₂O₄ spinel) B_0 differs (around 5%) from the common value of ~ 200 GPa obtained in the direct spinels.

IV. CONCLUSIONS

Analytical expressions connecting crystalline and polyhedral bulk moduli in spinels have been developed. Their capability to explain pressure effects on oxide direct and inverse spinels has been illustrated by the analysis of quantum mechanical results in AB₂O₄ (A :Mg,Zn; B :Al,Ga) crystals. Computed structural and compression data describe reasonably the known and expected behavior of these compounds. From cation-oxygen bond lengths vs pressure curves, it is seen that bonds involving trivalent cations are stiffer than the ones involving divalent cations, the differences between cations in each group being smaller. It can be concluded that the polyhedral compressibility is more dependent on the oxidation state of the cation occupying the interstice. Variations of octahedral and tetrahedral bulk moduli due to the change of trivalent and divalent cations, respectively, are less than 5%.

The nature of the polyhedral linkages necessary to recover the crystal bulk modulus in the empirical scheme of Hazen and Finger¹ is substituted in our theoretical model by the knowledge of the pressure effect on the internal position u of the oxygen in the unit cell. It is seen that for these fully edge-linked structures, the u dependence on pressure does not contribute appreciably to the prediction of the macroscopic bulk moduli, and we can generate B_0 from $(B_0)_{\text{oct}}$ and $(B_0)_{\text{tet}}$ values. The microscopic analysis performed in this study helps to understand the uniform behavior shown by oxide spinels under hydrostatic pressure and encourages us to generalize our theoretical treatment to other, more complicated, crystal structures.

ACKNOWLEDGMENTS

Financial support from Spanish DGICYT, Projects No. PB96-0559 and BQU2000-0466, are gratefully acknowledged. J.M.R. and R.F. want to express their gratitude to the Ministerio de Educación y Cultura (SEUID) of Spain for financial support during their stay at Universidad Jaume I (Spain) and Michigan Technological University (USA), respectively.

¹R.M. Hazen and L.W. Finger, *J. Geophys. Res.* **84**, 6723 (1979).

²P.W. Bridgman, *Proc. Am. Acad. Arts Sci.* **58**, 165 (1923).

³O.L. Anderson and J.E. Nafe, *J. Geophys. Res.* **70**, 3951 (1965).

⁴D.L. Anderson and O.L. Anderson, *J. Geophys. Res.* **75**, 3494 (1970).

⁵R.J. Hill, J.R. Craig, and G.V. Gibbs, *Phys. Chem. Miner.* **4**, 317 (1979).

⁶L.W. Finger, R.M. Hazen, and A. Hofmeister, *Phys. Chem. Miner.* **13**, 215 (1986).

⁷M.B. Kruger, J.H. Nguyen, W. Cadwell, and R. Jeanloz, *Phys. Rev. B* **56**, 1 (1997).

⁸S. Asbrink, A. Waskowska, J. Staun Olsen, and L. Gerward, *Phys. Rev. B* **57**, 4972 (1998).

⁹S. Asbrink, A. Waskowska, L. Gerward, J. Staun Olsen, and E. Talik, *Phys. Rev. B* **60**, 12 651 (1999).

¹⁰V. Luaña and L. Pueyo, *Phys. Rev. B* **41**, 3800 (1990).

¹¹T. Yamanaka and Y. Takeuchi, *Z. Kristallogr.* **165**, 65 (1983).

¹²E. Clementi and C. Roetti, *At. Data Nucl. Data Tables* **14**, 177 (1974).

- ¹³J. Chakravorty and E. Clementi, *Phys. Rev. A* **39**, 2290 (1989), and references therein.
- ¹⁴M.A. Blanco, V. Luaña, and A. Martafin Pendás, *Comput. Phys. Commun.* **103**, 287 (1997).
- ¹⁵R. Franco, J.M. Recio, and L. Pueyo, *J. Mol. Struct.: THEOCHEM* **426**, 233 (1998).
- ¹⁶E. Francisco, J.M. Recio, M.A. Blanco, A. Martín Pendás, and A. Costales, *J. Phys. Chem. A* **102**, 1595 (1998).
- ¹⁷F. Birch, *Phys. Rev.* **71**, 809 (1947).
- ¹⁸P. Vinet, J.H. Rose, J. Ferrante, and J.R. Smith, *J. Phys.: Condens. Matter* **1**, 1941 (1989).
- ¹⁹R. Pandey, J.D. Gale, S.K. Sampath, and J.M. Recio, *J. Am. Ceram. Soc.* **82**, 337 (1999).
- ²⁰P. D'Arco, B. Silvi, C. Roetti, and R. Orlando, *J. Geophys. Res.*, **96**, 6107 (1991).
- ²¹M.M. Sinha, N.P. Singh, K. Prasad, and H.C. Gupta, *Phys. Status Solidi B* **190**, K27 (1995).